Available online at www.sciencedirect.com

ScienceDirect

Sensors and Actuators B 132 (2008) 449–460

SENSORS AND ACTUATORS B CHEMICAL

www.elsevier.com/locate/snb

Flexible parylene-based multielectrode array technology for high-density neural stimulation and recording

Damien C. Rodger [a,b,*], Andy J. Fong [a], Wen Li [a], Hossein Ameri [b], Ashish K. Ahuja [b], Christian Gutierrez [b], Igor Lavrov [c], Hui Zhong [c], Parvathy R. Menon [a], Ellis Meng [b], Joel W. Burdick [a], Roland R. Roy [c], V. Reggie Edgerton [c], James D. Weiland [b], Mark S. Humayun [b], Yu-Chong Tai [a]

[a] *California Institute of Technology, Pasadena, CA, USA*
[b] *University of Southern California, Los Angeles, CA, USA*
[c] *University of California, Los Angeles, CA, USA*

Available online 12 November 2007

Abstract

Novel flexible parylene-based high-density electrode arrays have been developed for functional electrical stimulation in retinal and spinal cord prosthetics. These arrays are microfabricated according to a single-metal-layer process and a revolutionary dual-metal-layer process that promises to meet the needs of extremely high-density stimulation applications. While in many cases thin-film platinum electrodes in parylene C would be sufficient, high surface-area platinum electroplating has been shown to extend the lifetime of stimulated electrodes to more than 430 million pulses without failing. Iridium electrode arrays with higher charge delivery capacity have also been fabricated using a new high-temperature stabilized parylene variant, parylene HT. In addition, a new heat molding process has been implemented to conform electrode arrays to approximate the curvature of canine retinas, and a chronic implantation study of the mechanical effects of parylene-based electrode arrays on the retina over a 6-month follow-up period has provided excellent results. Retinal stimulation from these parylene-based electrode arrays in an isolated tiger salamander preparation was shown to be comparable to light stimulation in terms of generation of action potentials in the inner retina. Finally, electrode arrays have also been implanted and tested on the spinal cords of murine models, with the ultimate goal of facilitation of locomotion after spinal cord injury; these arrays provide a higher density and better spatial control of stimulation and recording than is typically possible using traditional fine-wire electrodes. Spinal cord stimulation typically elicited three muscle responses, an early (direct), a middle (monosynaptic), and a late (polysynaptic) response, classified based on latency after stimulation. Stimulation at different rostrocaudal levels of the cord yielded markedly different muscle responses, highlighting the need for such high-density arrays.

Keywords: Artificial vision; BioMEMS; Biomimetic; MEA; Neural prosthesis; Parylene C; Parylene HT; Retinal prosthesis

1. Introduction

Low-electrode-density neural prostheses have shown incredible promise, enabling those with severe hearing impairments to recognize speech [1] and those blind from such devastating outer retinal diseases as retinitis pigmentosa (RP) (where the photoreceptors are damaged but the remaining inner retinal circuitry remains largely intact [2]) to perceive visual data [3]. Subjects with prototype sixteen-electrode retinal prostheses can even distinguish between objects such as plates, cups, and knives, and perceive directions of movement in high-contrast environments far better than would be possible by chance alone [4]. However, there exists a need for a multielectrode array (MEA) technology that is capable of increasing the density of neural stimulation beyond its current limits, while ensuring biocompatibility and device longevity. In fact, for retinal stimulation in particular, it has been shown that room navigation could be significantly improved with an electrode array comprising one thousand or more electrodes, and furthermore such an array would likely enable facial recognition and large type reading [5]. The next-generation retinal prosthesis for patients with diseases like RP and age-related macular degeneration (AMD) (Fig. 1), then, requires a high-density flexible electrode array

* Corresponding author at: California Institute of Technology, Department of Bioengineering, 1200 E. California Building, M/C 136-93, Pasadena, CA 91125, USA. Tel.: +1 626 395 8477; fax: +1 626 584 9104.
E-mail address: dcrodger@mems.caltech.edu (D.C. Rodger).

0925-4005/$ – see front matter
doi:10.1016/j.snb.2007.10.069

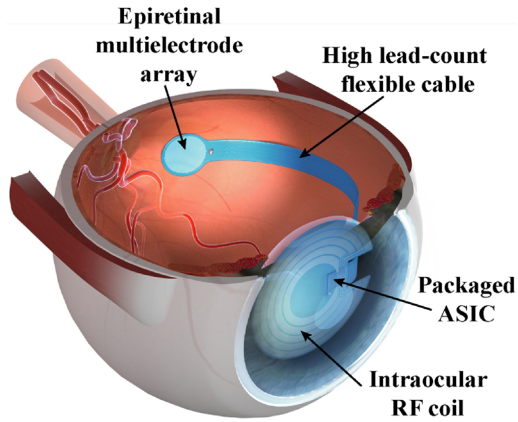

Fig. 1. Placement and components of envisioned next-generation intraocular retinal prosthesis.

capable of stimulating the inner retina and a high-lead-count cable to allow for high-resolution vision. We present the first flexible parylene-based MEAs designed for functional electrical stimulation in retinal prostheses, and the extension of this technology to enable stimulation of central nervous system structures after spinal cord injury. In addition to presenting a high surface-area electroplating technology that extends stimulation electrode longevity to at least 430 million pulses, which is ample for many applications, we address the importance of a novel parylene-enabled dual-metal-layer fabrication methodology that permits complex electrode arrangements while alleviating the traditional problems of electrode crowding and electrode size restrictions caused by wire routing. Promising chronic biomechanical stability results in canine eyes and acute neural recording and stimulation results in an *in vitro* retinal preparation and *in vivo* in murine spinal cords are presented, demonstrating the ability of these parylene-based arrays to both record from and stimulate the neuronal targets of interest. All animal procedures conformed to the ARVO Statement on the Use of Animals in Ophthalmic and Vision Research.

The advantages of using parylene C as the structural material for such neuroprostheses, when compared with technologies based on the use of other materials such as PDMS, polyimide [6] and silicon [7], include parylene's pinhole-free conformality due partly to its unique room-temperature chemical vapor deposition process, its low water permeability, its chronic implantability as an ISO 10993, United States Pharmacopeia (USP) Class VI material (highest biocompatibility class for plastics in the United States), and its high flexibility and mechanical strength (Young's modulus ∼4 GPa). Since parylene is deposited at room temperature (we have verified this using Temp-Plate irreversible temperature recorders traceable to NIST (Wahl Instruments, Inc., Asheville, NC, USA)), the coating process is post-integrated-circuit (IC) compatible. Parylene C is also optically transparent, enabling the anatomy to be seen through the cable and the array during ophthalmic surgery, post-implantation examination, and follow-up. While many groups use parylene C as a coating of their arrays for many of these reasons, we have chosen to use it as the main substrate for our devices [8,9], a paradigm that leverages these advantages to the greatest extent. A new high-temperature stable [10] and ISO 10993 biocompatible [11–13] fluorinated variant of parylene, parylene HT, that is similar in many respects to parylene C, has also been used to fabricate iridium electrode arrays. We show that while evaporation and patterning of iridium was unsuccessful on parylene C due to the high melting temperature of iridium, parylene HT lends itself to such a process, and we present this as another possible technology for ensuring good charge delivery to neural tissue.

2. Fabrication methods

2.1. Single-layer process

Single-metal-layer parylene C-based electrode arrays are fabricated as shown in Fig. 2. A photoresist sacrificial layer is optionally spun on a standard silicon wafer. Approximately 8 μm of parylene C is then vapor-deposited in a PDS2010 system (Specialty Coating Systems, Indianapolis, IN, USA) on the entire wafer. An LOR3B photoresist layer (Microchem Corporation, Newton, MA, USA) and an AZ1518 layer (AZ Electronic Materials, Branchburg, NJ, USA) are spun on top of the parylene, exposed in a 10× reduction GCA Mann 4800 DSW wafer stepper (General Signal Corporation, Stamford, CT, USA) or a Kasper 2001 contact aligner (Kasper Instruments, Inc., Sunnyvale, CA, USA) depending on the required resolution of the electrode array, and developed to achieve a liftoff pattern consisting of contacts, conductive traces, and electrodes. After hard-bake, approximately 2000–5000 Å of platinum, with or without a 200 Å titanium layer, is then e-beam evaporated (SE600 RAP, CHA Industries, Fremont, CA, USA) on the wafer. The subsequent photoresist strip generates the desired single-layer metallization pattern. An approximately 7-μm-thick coating of parylene C is then deposited, followed by a spin coating of photoresist. This photoresist etch mask is exposed over the areas of the electrodes and contact pads and to pattern the overall array geometry, and the entire wafer is then subjected to a reactive-ion etch in oxygen plasma, removing the parylene insulation over the electrodes and the parylene surrounding the array. The photoresist mask is then removed with solvent. Finally, if a sacrificial photoresist layer was used, the array is released from the substrate in an acetone bath. If no sacrificial layer was used, it is peeled from the silicon in a water bath. Ultimately, for most cases, the sacrificial photoresist layer is unnecessary.

Due to the higher thermal stability of parylene HT (long-term stability at 350 °C, intermittent exposures up to 450 °C [12]), it was surmised that the material would be better suited to iridium array fabrication than would parylene C (the melting temperature of iridium is 2447 °C whereas that of platinum, for which a parylene C substrate works well, is 1772 °C [14]). Consequently, a minor modification of this process is made to fabricate iridium electrode arrays. A thin parylene C layer (∼2.4 μm) is deposited on the silicon wafer followed by a thicker layer of parylene HT (∼5.7 μm) in a PDS2035 system (Specialty Coating Systems). The parylene C layer facilitates fabrication and subsequent release, whereas the HT layer provides the necessary thermal stability. The dual photoresist layer is spun and patterned, and the

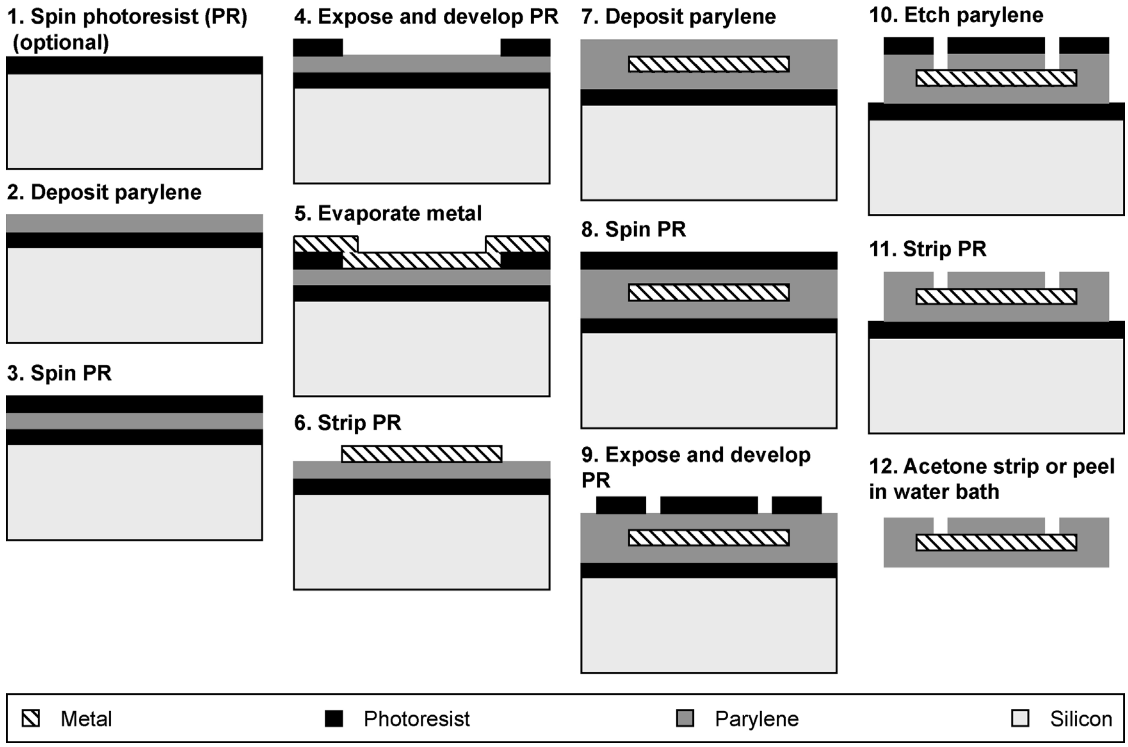

Fig. 2. Fabrication process for parylene-based single-metal-layer MEAs. A simple modification of this process is required for iridium electrode array fabrication.

iridium (~800 Å) is then e-beam evaporated on the wafer. After liftoff, a final parylene HT layer (~5.4 μm) is deposited and patterned as with the parylene C arrays, and the arrays are released in a water bath. This process was compared to an identical process performed using only parylene C structural layers.

2.2. Dual-layer process

Dual-metal-layer electrode arrays are fabricated as shown in Fig. 3. Approximately 8 μm of parylene C is first deposited on a silicon wafer with the optional photoresist sacrificial layer,

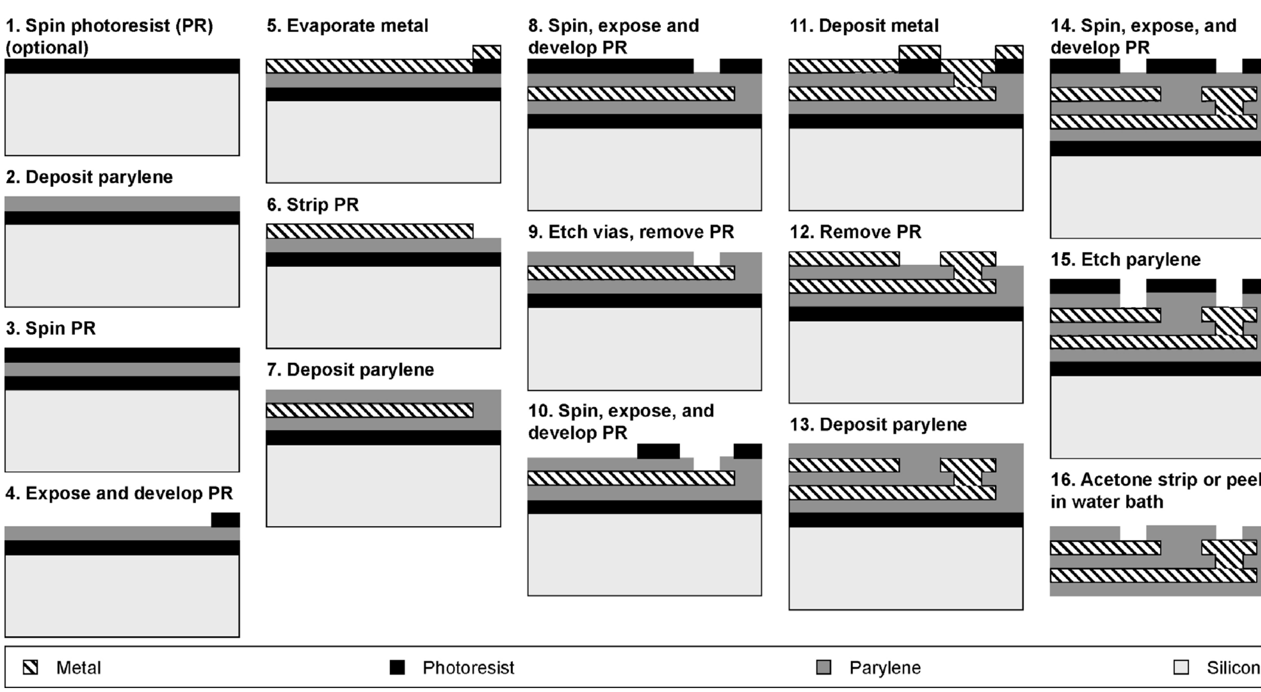

Fig. 3. Fabrication process for parylene-based dual-metal-layer MEAs.

forming the underside of the electrode array. A platinum or titanium–platinum metal liftoff process is used to define traces with 16 μm pitch and 2000–3000 Å thickness. A second parylene deposition (∼1 μm) forms the insulation between the two metal layers. At this point, 6 μm × 6 μm vias are patterned in the insulation layer over the ends of the traces using an O_2 plasma reactive-ion etch. A second step-coverage optimized liftoff process is used to define a second metal layer comprising electrodes and traces, while at the same time achieving electrical continuity between the underlying traces and the overlying electrodes. A final parylene coating approximately 7 μm thick forms the top insulation. The electrodes are exposed and the overall geometry of the implant is defined in a final set of O_2 reactive-ion etches using a thick photoresist etch mask. Finally, the arrays are peeled from the wafer in a water bath or released through removal of the sacrificial photoresist in acetone.

2.3. Annealing and heat molding

The implants are typically annealed for 2 days at 200 °C in a vacuum oven with nitrogen backfill to optimize parylene–parylene adhesion. Under accelerated-lifetime passive soak test conditions, such an annealing process has been shown to increase the extrapolated mean time to failure of devices to 20 years or more [9]. In addition, an important aspect of these parylene arrays is that they are heat moldable. If the arrays are contoured and confined to a geometry of interest for the target application during this annealing process, we have discovered that this conformation will be maintained during sterilization, implantation, and follow-up. In order to maintain the planarity of the spinal cord arrays during annealing, they are clamped between two flat pieces of Teflon or glass slides coated with aluminum foil. The retinal arrays, on the other hand, are shaped using a custom 6061 aluminum mold comprising a recessed concave region and a mating stainless steel sphere that approximates the curvature of the retina. During annealing, the array region is sandwiched between the sphere and the mating surface, while the cable is pressed flat against an aluminum plateau.

2.4. Electroplating

As a possible mechanism for extending the longevity of chronically pulsed electrodes, we are investigating electroplated films of high surface-area platinum. Specially designed thin-film platinum electrode arrays, consisting of sixteen 150-μm-diameter electrodes of 3000 μm center-to-center spacing, were fabricated according to the single-layer process. They were immersed in an aqueous ammonium hexachloroplatinate solution in a specialized jig and six were plated according to Whalen et al. [15] at a plating potential of −0.6 V (vs. an Ag/AgCl reference electrode) for 1.5 h. The others remained unplated. Electrochemical tests were performed to evaluate the efficacy of this plating step in extending electrode longevity under chronic pulsing.

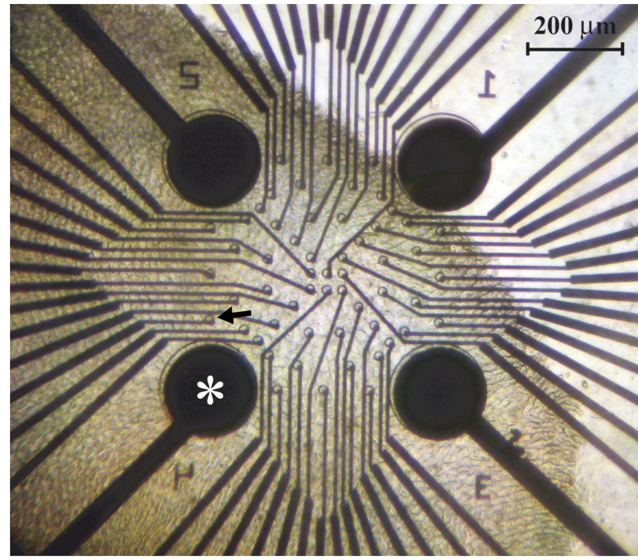

Fig. 4. Isolated larval tiger salamander retina (darker region) overlying parylene-based platinum electrode array. Arrow indicates 10-μm-diameter electrode used for recording traces in Figs. 5 and 6. Asterisk identifies 200-μm-diameter stimulating electrode used to generate action potentials seen in Fig. 6.

3. Results and discussion

3.1. In vitro retinal recording and stimulation

Parylene C-based arrays of thin-film platinum electrodes, comprising four 200-μm-diameter stimulating electrodes and 56 recording electrodes of 10 μm diameter were fabricated according to the single-metal-layer process on a glass substrate. These were placed in a bicarbonate perfusate under a microscope and connected to a stimulus generator and preamplification board (Multi Channel Systems MCS GmbH, Reutlingen, Germany) [16]. As shown in Fig. 4, a retina isolated from larval tiger salamander (*Ambystoma tigrinum*) was placed retinal ganglion cell side down on the array (to simulate epiretinal stimulation), and a remote platinum ground electrode was introduced to the bath. In order to assess retinal health, and for comparison with electrical stimulation results, a white light pulse 40 ms in duration was applied to the tissue. As shown in Fig. 5, a voltage trace of the activity of the cells overlying one of the recording electrodes (electrode indicated with an arrow in Fig. 4), a robust ON response was detected after the phototransduction delay, followed by the expected OFF response ∼50 ms later. Subsequently, with the lights off, a 20 μA, 400 μs/phase, cathodic-first biphasic electrical pulse was applied between the stimulating electrode indicated with an asterisk in Fig. 4 and the ground electrode. The voltage trace from the same recording electrode as before is shown in Fig. 6. This stimulation was consistently repeatable over a 50 pulse train with a 400 ms interpulse interval, and other stimulating electrodes were also capable of "epiretinally" stimulating other cells in the retinal slice. As is clear from these results, the parylene-based platinum electrode was able to stimulate the tissue and elicit a response similar to the response generated from a light pulse in this intact retina. Given these results and the knowledge garnered from clinical

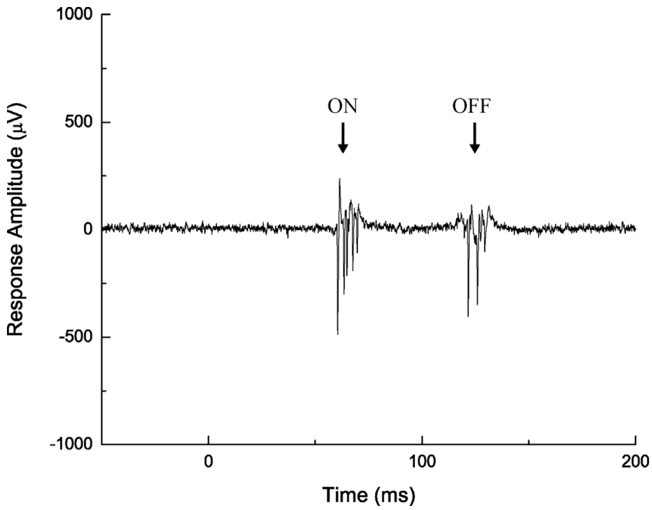

Fig. 5. Recording of ON response followed by OFF response of cells overlying electrode denoted with an arrow in Fig. 4 to a full-field white light stimulus of 40 ms duration. Pulse began at 0 ms on the abscissa, with delay until ON response due to phototransduction.

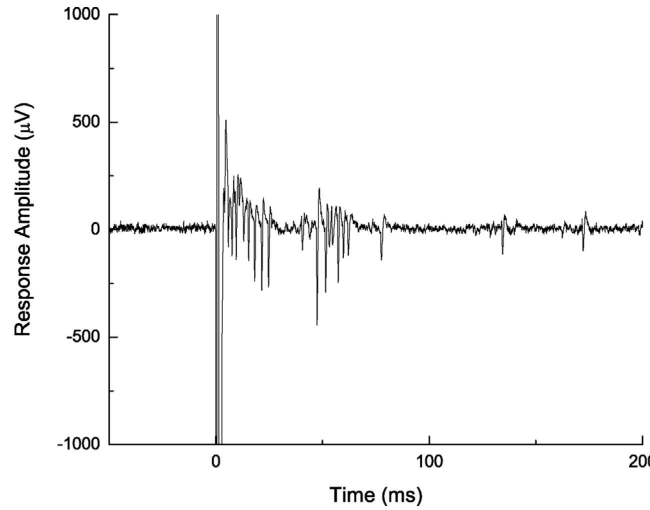

Fig. 6. Typical recording of response of cells overlying same recording electrode as in Fig. 5 to a 20 μA, 400 μs/phase, cathodic-first biphasic electrical pulse from "epiretinal" stimulating parylene-based platinum electrode denoted with an asterisk in Fig. 4. Spike at 0 ms on abscissa is stimulation artifact.

trials with prototype arrays fabricated of other materials, it is not unreasonable to presume that our arrays will most likely be able to stimulate retinal tissue in other species, including human. To this end, the chronic biostability of implanted parylene-based arrays was also evaluated.

3.2. Chronic retinal implantation

Chronically implantable retinal electrode arrays comprising 1024, 75-μm-diameter electrodes arranged in a complex biomimetic pattern that closely mimics the density of ganglion

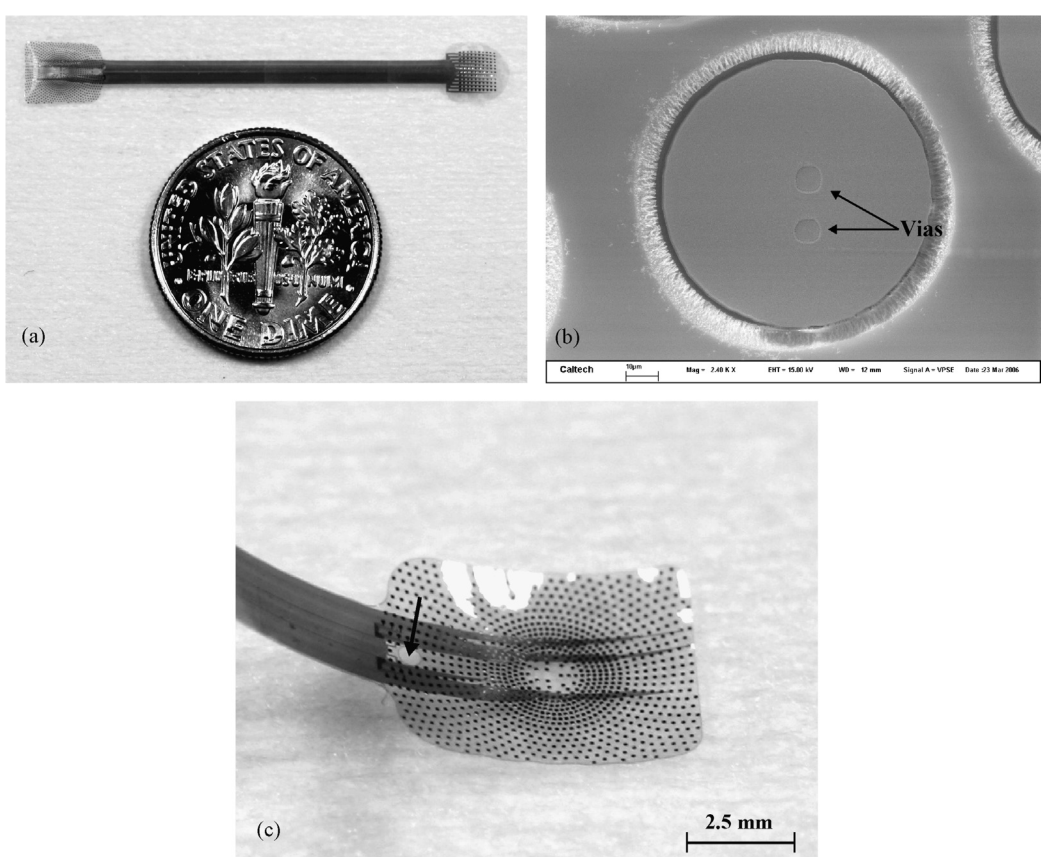

Fig. 7. (a) Fabricated biomimetic electrode array with 60 of 1024 75-μm-diameter electrodes connected through dual-layer process with U.S. dime for size comparison; (b) SEM of electrode highlighting vias to underlying traces; (c) heat molded and annealed retinal electrode array with retained spherical curvature (arrow denotes retinal tack hole).

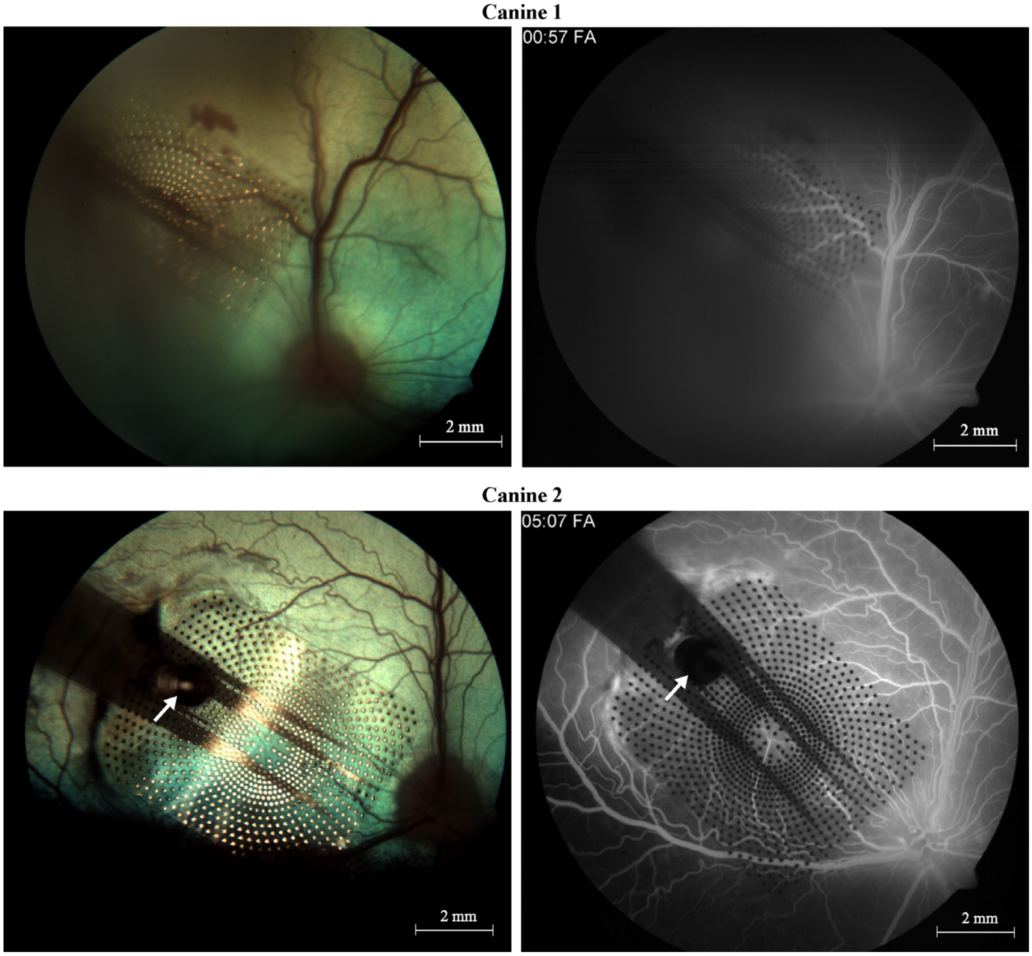

Fig. 8. Fundus photographs (left) showing parylene MEAs tacked to the right retina of both animals and FAs (right) showing normal vessel perfusion under the arrays. Arrows point to retinal tack.

cells in the human retina [17] were fabricated according to the dual-layer process (Fig. 7a), with 60 of the electrodes connected via two traces each to facilitate electrical conductivity verification. The strength of metal adhesion was verified using a Scotch tape test, which demonstrated that direct platinum evaporation is feasible without the need for a titanium adhesion layer. Electrical testing demonstrated a typical impedance of approximately 5 kΩ, which includes two 8-μm-wide traces of 20 mm length, as well as two via step junctions connecting underlying traces to the overlying electrode (vias are shown in Fig. 7b, a scanning electron micrograph (SEM) of a single electrode). Each via had an impedance of less than 12.5 Ω. These arrays were successfully molded to the approximate curvature of the canine retina (Fig. 7c) using the custom mold, and sterilized using ethylene oxide gas.

Our biomimetic arrays were implanted in the right eye of two canines through a 5-mm pars plana incision after vitrectomy, and were affixed to the retina using a retinal tack modified by the addition of a PDMS washer (to account for the thin nature of the parylene-based arrays). Follow-up in both animals was conducted for 6 months using fundus photography, fluorescein angiography (FA), in which blood is fluorescently stained to assess vessel perfusion in the retina, and optical coherence tomography (OCT), an interferometric technique that enables cross-sectional imaging of the retina. Fundus photography and FAs of both animals, examples of which are shown in Fig. 8, consistently demonstrated that vessel filling underneath the array was normal. Obstruction and vessel leakage would have been visualized if the array were placing excessive pressure on the retina. In addition, OCT demonstrated that the electrodes were consistently less than 50 μm away from the ganglion cell layer in both animals (typical OCTs of both animals are shown in Fig. 9), an outcome that theoretically affords excellent electrical coupling between the electrodes and the electrically excitable cells of the retina. It is important to note that in the OCT of the second canine, the scan was taken along a segment furthest from the tack site, where one might expect the least proximity. Even at this location, this array remained in very close apposition throughout the 6-month implantation. Post-enucleation histology has since confirmed the excellent biostability seen during follow-up.

The dual-metal-layer process is wholly enabled by the use of parylene as an insulating layer. The low dielectric constant of parylene (∼3.1 at 1 kHz [13]) enables this layer to be very thin while still minimizing capacitive crosstalk between overlapping and adjacent metal lines. The vapor-deposition process

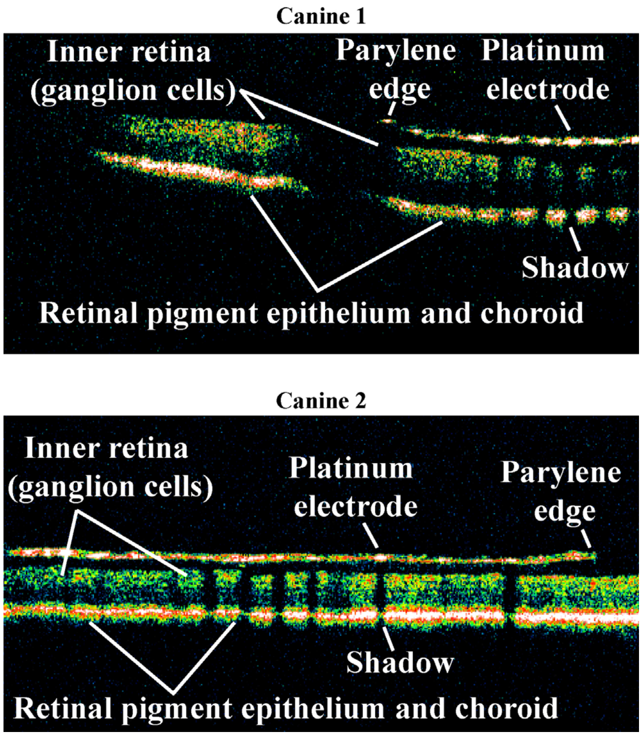

Fig. 9. OCTs of both animals showing very close apposition (<50 μm) of the arrays to the retinal ganglion cell layer.

for parylene ensures that this layer can remain thin while still being pinhole free, where a spin-on coating, on the other hand, would prove problematic. The process depends on optimal step-coverage of the parylene sidewall during evaporation, which is aided, in part, by the slightly isotropic nature of the O_2 plasma etch of parylene [18]. The dual-layer process proffers considerable advantages over the more traditional single-layer approach. Design of single-layer electrode arrays is usually hindered by the need to route traces amongst the electrodes. This tends to cause crowding of traces and electrodes into groups, an organization that may not be optimal for stimulating the tissue of interest. In addition, this has a propensity to constrain the geometric area of the electrodes in the MEAs to smaller sizes, and thus reduces the number of electrodes possible in a given area. The dual-layer process obviates these problems by enabling traces to pass under overlying electrodes without making contact to them, having the effect of both relaxing the constraints on electrode size and number and enabling more complex electrode organization (such as the biomimetic one presented in this work). Although the arrays fabricated here had just 60 electrodes of connectivity with 120 traces total, this was without making full use of both layers for wire routing and connection of electrodes. In order to not make traces unnecessarily narrow and of too high impedance, we believe an extension of this process to three or more metal layers will be necessary to achieve 1024 electrodes of total connectivity. Indeed, this fabrication process is easily extendable to such structures through the addition of extra layers of parylene and metal. Given the encouraging biostability results presented here and the ability of these arrays to stimulate retinal tissue, future studies will include chronic

Fig. 10. Parylene MEA for murine spinal cord stimulation and recording.

stimulation with implanted parylene-based arrays in an animal model.

3.3. In vivo spinal cord recording and stimulation

Spinal cord arrays, consisting of five or ten electrodes of 250 μm diameter (Fig. 10), were fabricated using the single-layer process. Interelectrode spacing was controlled so that each array covered four to five segments of the lumbosacral spinal cord. These were connected via Clincher connectors (FCI, Versailles Cedex, France) to the stimulation and recording electronics.

Under isoflurane anesthesia, the spinal cord electrode arrays were implanted epidurally on spinal cord segments L2-S1 in nontransected mice. The electrodes were oriented linearly along the rostrocaudal extent of the cord. Recording capability was assessed by using the electrode array to record spinal cord potentials evoked by tibial nerve stimulation. Following stimulation of the tibial nerve, somatosensory evoked potentials were recorded from the cord dorsum at three lumbosacral levels (P1–P3, rostral to caudal). The recorded waveform consisted of three response peaks, two of which are clearly depicted in Fig. 11 (N1 and N3). These findings closely mirror results reported previously in a

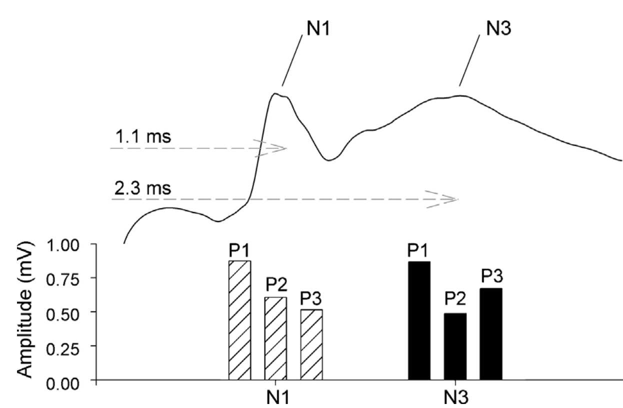

Fig. 11. Peak amplitudes of somatosensory evoked potentials (N1 and N3) recorded from three levels of the rostrocaudal spinal cord (P1–P3). Example waveform at top shows approximate response times.

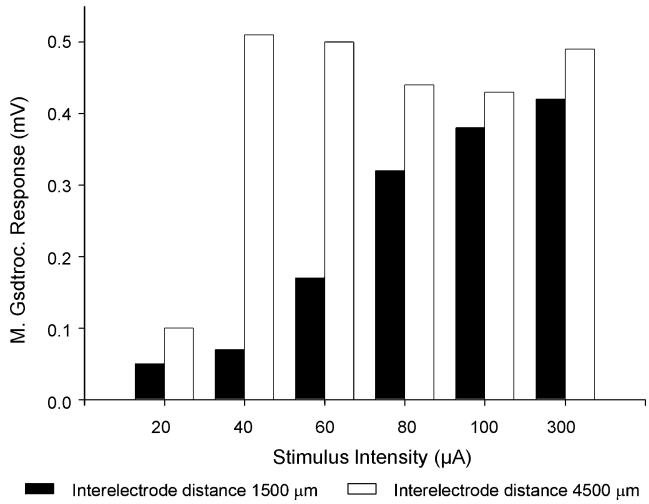

Fig. 12. Effect of interelectrode spacing on muscle recruitment. Smaller spacings yielded graded muscle activation while larger spacings yielded maximal amplitude responses at low currents.

study using conventional spinal cord recording electrodes [19] demonstrating that the recording capability of the array electrodes matches that of conventional electrodes. By measuring the difference in the response latencies obtained at each electrode position (corresponding to different levels of the spinal cord), and by utilizing the known, fixed interelectrode spacing, accurate measurements of the conduction velocities were obtained. The properties of these responses can potentially be used to diagnose the progressive recovery of the spinal cord as a result of treatments provided after a spinal cord injury.

To test the capability of the electrode array to act as a multi-channel stimulating device for generating hindlimb movements, constant-current monophasic stimulus pulses (amplitude: 50–850 μA, frequency: 0.3–10 Hz, pulse duration: 0.5 ms) were applied to the spinal cord between each of the array electrodes and a ground electrode located near the shoulder, while muscle activity was monitored using electromyogram (EMG) recordings of the tibialis anterior and medial gastrocnemius muscles. Stimulation generated a typical three-component EMG action potential consisting of an early (direct motor), a middle (monosynaptic), and a late (polysynaptic) response, classified by post-stimulus latency. The appearance and magnitude of each of these responses was correlated with the choice of electrode position and stimulation parameters. Varying the interelectrode spacing between the stimulating electrode and a ground electrode now on the array affected the sensitivity with which the target muscles were activated. The recruitment profile of the medial gastrocnemius middle response is shown in Fig. 12 using interelectrode spacings of 1500 μm (filled bars) and 4500 μm (unfilled bars). Using the smaller spacing, graded muscle activation was achieved. With the larger spacing, approaching a monopolar configuration, the muscle quickly attained maximal activation at low currents. Thus, the specific goal and sensitivity requirements of a particular motor task may dictate optimal interelectrode spacing and whether a monopolar or bipolar configuration is chosen. Currently, we are developing higher-density MEAs capable of bilateral stimulation for assessing the somatotopic distribution of locomotor circuits in the spinal cord.

3.4. Thin-film vs. electroplated platinum

The ability of the electroplating process to extend electrode longevity was evaluated by chronically pulsing single-layer thin-film and platinum-plated electrodes in PBS. Cyclic voltammograms (CVs) were performed in 250 mM aqueous sulphuric acid prior to plating and periodically during pulsing to estimate electrode surface area and overall electrode health. In addition, voltage responses to the current pulses were recorded and electrochemical impedance spectroscopy (EIS) was performed regularly. The plated and unplated electrodes were pulsed continuously for 50 days, or until failure occurred, at 100 Hz with a

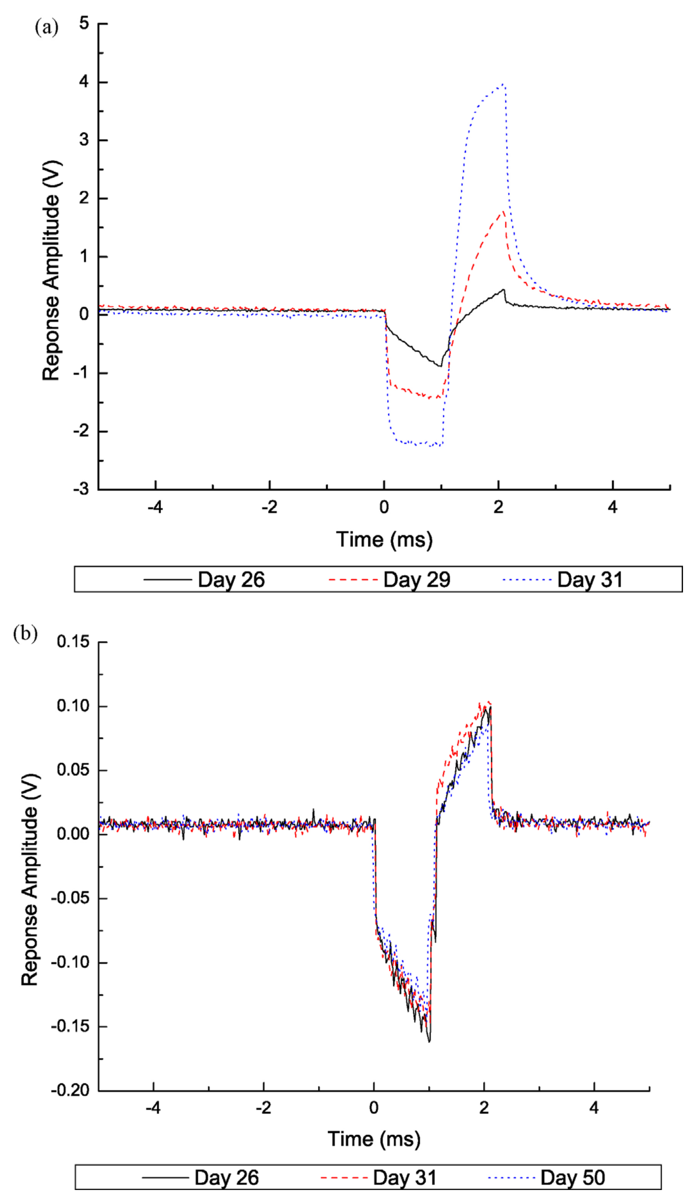

Fig. 13. Voltage responses to a current pulse for (a) an unplated electrode, documenting the process of electrode failure, and (b) a plated electrode, showing steady responses throughout the 50-day test.

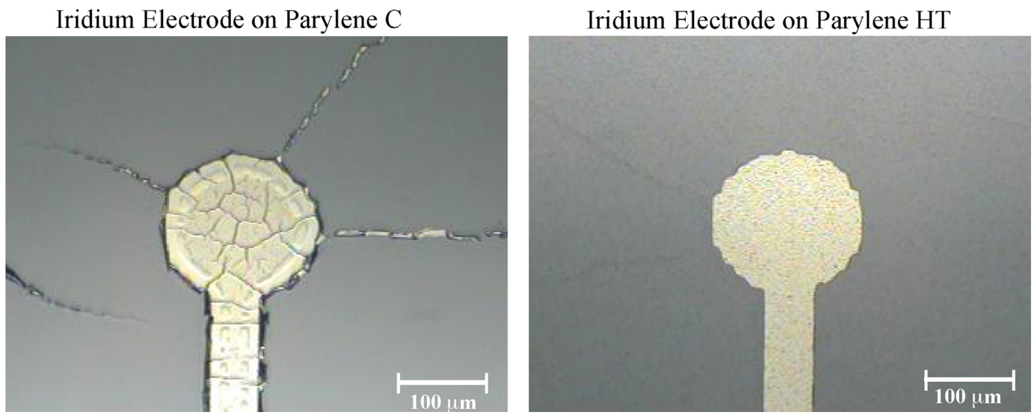

Fig. 14. Photomicrograph of an iridium electrode on a parylene C surface after liftoff (left) compared with an iridium electrode on a parylene HT surface after liftoff (right). Parylene HT enables fabrication of flexible iridium electrode arrays through thermal evaporation.

60 μA (~0.34 mC/cm^2 of geometric electrode area, close to the upper limit of charge density for platinum, typically considered to be 0.35 mC/cm^2 [20]) biphasic cathodic-first current pulse with 1 ms per phase and a 100 μs inter-phase delay.

The estimated surface area of the electrodes (determined by comparing the areas under the hydrogen desorption peaks in the CVs) increased approximately 40–50 times between before and after plating. Under pulsing, the voltage responses of both plated and unplated electrodes remained stable for approximately 29 days, at which point the unplated electrodes showed signs of failure. Voltage responses for one such electrode on day 26, 29, and 31 are overlaid in Fig. 13a, which documents the progression of failure. The plated electrodes, on the other hand, remained intact for much longer, most surviving more than 50 days, or 430 million pulses, at which point the testing goal was met and the test was stopped (overlaid voltage responses for one such electrode, showing the voltage responses at day 26, 31, and 50, are shown in Fig. 13b). In addition, the electrochemical impedance magnitudes at 1 kHz of a typical plated and unplated electrode averaged approximately 1.2 and 4.4 kΩ, respectively for the 3 weeks of testing. A dramatic jump in impedance to approximately 0.87 MΩ was observed for the unplated electrode at the time of failure (approximately day 29), while the plated electrode demonstrated only minor variability in its low impedance throughout the 430-million-pulse trial. These preliminary data corroborate the evidence that plating of the electrodes is beneficial to longevity, and suggest that high surface-area platinization of electrodes can have a dramatic effect on extending electrode life, while lowering electrochemical impedance to charge delivery. Future work will include replication of these tests and chronic pulsing at high temperatures for longer times to further accelerate and assess the possible modes of failure.

3.5. Iridium electrode arrays

While the charge delivery capacity of platinum is sufficient for many applications, that of iridium is significantly higher [21], as it has four oxidation states as opposed to two [22]. In addition, iridium can be cycled to form an activated iridium oxide film (AIROF) [23] with even higher charge delivery capacity. Our investigation into the possibility of fabricating parylene-based flexible iridium electrode arrays spawned from such considerations. Usually, iridium or iridium oxide are deposited through sputtering [22,24] or electroplating [25,26], especially when they are applied to flexible substrates, a likely reason being that the high melting-temperature of the material makes evaporation on polymers quite foreboding (thermal evaporation on thermally conductive substrates such as silicon is possible, however [27]).

Our comparison of iridium array fabrication on parylene C and fabrication on parylene HT yielded remarkable results. As can be seen in Fig. 14, when e-beam evaporated and patterned on parylene C, the iridium film cracked and the liftoff was incomplete. Electrically, the traces from the contacts to the electrodes were non-conductive. However, when the arrays were fabricated using the hybrid parylene C/HT process, the evaporation and liftoff on the HT surface occurred routinely (Fig. 14). In addition, electrical testing of contact-electrode-contact circuits using sets of 45-μm-wide traces ranging 56–70 mm in length revealed impedances ranging from approximately 12.8–16.7 kΩ, depending on the lengths of the traces in the circuit (the high resistance is due to the thin nature of the iridium wires). An SEM

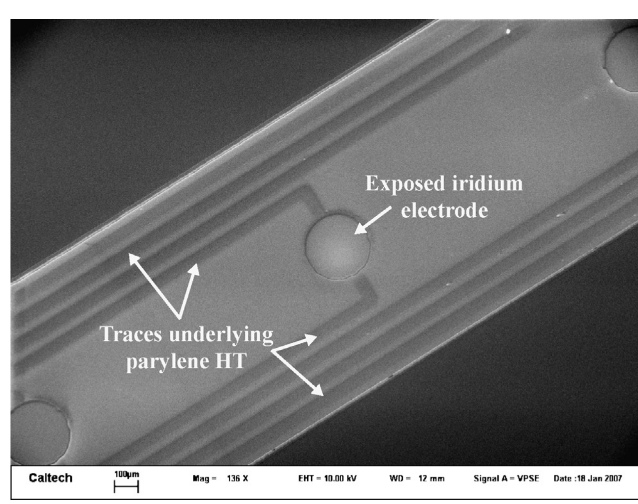

Fig. 15. SEM of a fabricated parylene HT-based iridium MEA. Compositional analysis through EDS verified exposed material as iridium.

of a fabricated parylene HT-based iridium electrode array is shown in Fig. 15. The composition of the electrode surface was analyzed via energy dispersive spectroscopy (EDS) and verified to be iridium. This work constitutes, to our knowledge, the first time that iridium electrode arrays have been successfully fabricated on a parylene substrate through thermal evaporation. Future work includes electrochemical analysis and chronic pulsing of these and similarly fabricated iridium arrays.

4. Conclusion

Single and dual-metal-layer fabrication processes for parylene-based electrode arrays have been outlined and demonstrated as robust techniques for building flexible MEAs. These revolutionary MEAs have the ability to stimulate and record from neural tissue in the retina and spinal cord, and demonstrate excellent biostability when chronically implanted in contact with canine retinas. The parylene-enabled dual-metal-layer process allows increased electrode density while obviating many of the issues typically associated with single-layer arrays, such as constraints on electrode size and electrode crowding due to wire routing. It is a simple matter to extend this process to increase the number of metal and parylene insulation layers, as will likely be necessary to fabricate a fully connected 1024-electrode device of approximately the same geometry. High surface-area platinum electroplating technology has shown encouraging results in terms of extending electrode life while also decreasing electrochemical impedance. In addition, evaporated iridium electrode arrays have been fabricated using a novel high-temperature stable variant of parylene, parylene HT, further adding to the repertoire of parylene-based technologies for retinal, spinal, and other neural interfaces.

Acknowledgments

This work was supported in part by the Engineering Research Centers Program of the National Science Foundation under NSF Award Number EEC-0310723, and by a fellowship from the Whitaker Foundation (D.R.). The authors especially wish to thank Dr. Jack Whalen and Ms. Aditi Ray for their help with the electroplating and electrochemical testing experiments, Dr. Saloomeh Saati for her help with the *in vivo* canine studies, Mr. Matthew Behrend for his work on the isolated retina setup, Ms. Ronalee Lo for her help with the fabrication of the PDMS washers used with the retinal tacks, Mr. Andrew Pullin for his help with fabrication of the heat-forming mold, and Mr. Trevor Roper for his always valuable assistance.

References

[1] B.S. Wilson, C.C. Finley, D.T. Lawson, R.D. Wolford, D.K. Eddington, W.M. Rabinowitz, Better speech recognition with cochlear implants, Nature 352 (1991) 236–238.

[2] E. Margalit, S.R. Sadda, Retinal and optic nerve diseases, Artif. Organs 27 (2003) 963–974.

[3] M.S. Humayun, J.D. Weiland, G.Y. Fujii, R. Greenberg, R. Williamson, J. Little, B. Mech, V. Cimmarusti, G. Van Boemel, G. Dagnelie, Visual perception in a blind subject with a chronic microelectronic retinal prosthesis, Vis. Res. 43 (2003) 2573–2581.

[4] J.D. Weiland, D. Yanai, M. Mahadevappa, R. Williamson, B.V. Mech, G.Y. Fujii, J. Little, R.J. Greenberg, E. de Juan Jr., M.S. Humayun, Visual task performance in blind humans with retinal prosthetic implants, in: Tech. Digest, Int. IEEE Eng. in Med. and Biol. Soc. Meet., San Francisco, CA, USA, September 1–5, 2004.

[5] J.D. Weiland, W. Liu, M.S. Humayun, Retinal prosthesis, Annu. Rev. Biomed. Eng. 7 (2005) 361–401.

[6] T. Stieglitz, W. Haberer, C. Lau, M. Goertz, Development of an inductively coupled epiretinal vision prosthesis, in: Tech. Digest, Int. IEEE Eng. in Med. and Biol. Soc. Meet, San Francisco, CA, USA, September 1–5, 2004.

[7] A.C. Hoogerwerf, K.D. Wise, A three-dimensional microelectrode array for chronic neural recording, IEEE Trans. Biomed. Eng. 41 (1994) 1136–1146.

[8] D.C. Rodger, J.D. Weiland, M.S. Humayun, Y.-C. Tai, Scalable high lead-count parylene package for retinal prostheses, Sens. Actuators B: Chem. 117 (2006) 107–114.

[9] W. Li, D.C. Rodger, E. Meng, J.D. Weiland, M.S. Humayun, Y.-C. Tai, Flexible parylene packaged intraocular coil for retinal prostheses, in: Tech. Digest, Int. IEEE-EMBS Microtech. in Med. and Bio. Meet., Okinawa, Japan, May 9–12, 2006.

[10] R. Kumar, D. Molin, L. Young, F. Ke, New high temperature polymer thin coating for power electronics, in: Tech. Digest, APEC Meet, Anaheim, CA, USA, February 22–26, 2004.

[11] L. Wolgemuth, Crystal-clear coating covers components, Med. Des. 6 (2006) 48–51.

[12] http://www.scscoatings.com/news/press_parylene-ht.cfm (accessed: June 24, 2007).

[13] http://www.sensorsexpo.com/exbdata/6698/brochures/SCS%20Electronic%20Coatings.pdf (accessed: June 24, 2007).

[14] P.W. Atkins, General Chemistry, Scientific American Books, New York, 1989.

[15] J.J. Whalen, J.D. Weiland, P.C. Searson, Electrochemical deposition of platinum from aqueous ammonium hexachloroplatinate solution, J. Electrochem. Soc. 152 (2005) C738–C743.

[16] A.K. Ahuja, M.R. Behrend, M. Kuroda, M.S. Humayun, J.D. Weiland, Spatial response properties of electrically stimulated retina, Invest. Ophthalmol. Vis. Sci. 48 (2007) 4444.

[17] C.A. Curcio, K.A. Allen, Topography of ganglion-cells in human retina, J. Comp. Neurol. 300 (1990) 5–25.

[18] E. Meng, Y.-C. Tai, Parylene etching techniques for microfluidics and bioMEMS, in: Tech. Digest IEEE Int. Conf. on MEMS Meet., Miami, FL, USA, January 30–February 3, 2005.

[19] A.P. Chandran, K. Oda, H. Shibasaki, M. Pisharodi, Spinal somatosensory evoked potentials in mice and their developmental changes, Brain Dev. 16 (1994) 44–51.

[20] S.B. Brummer, M.J. Turner, Electrical stimulation with Pt electrodes: II-estimation of maximum surface redox (theoretical non-gassing) limits, IEEE Trans. Biomed. Eng. 24 (1977) 440–443.

[21] W. Mokwa, MEMS technologies for epiretinal stimulation of the retina, J. Micromech. Microeng. 14 (2004) S12–S16.

[22] E. Slavcheva, R. Vitushinsky, W. Mokwa, U. Schnakenberg, Sputtered iridium oxide films as charge injection material for functional electrostimulation, J. Electrochem. Soc. 151 (2004) E226–E237.

[23] L.S. Robblee, J.L. Lefko, S.B. Brummer, Activated Ir—an electrode suitable for reversible charge injection in saline solution, J. Electrochem. Soc. 130 (1983) 731–733.

[24] M.A. El Khakani, M. Chaker, B. Le Drogoff, Iridium thin films deposited by radio-frequency magnetron sputtering, J. Vacuum Sci. Technol. A-Vacuum Surf. Films 16 (1998) 885–888.

[25] J.D. Weiland, S. Cogan, M.S. Humayun, Micro-machined, polyimide stimulating electrodes with electroplated iridium oxide, in: Tech. Digest, Int. IEEE Eng. in Med. and Biol. Soc. Meet, Atlanta, GA, USA, October 13–16, 1999.

[26] R.D. Meyer, S.F. Cogan, T.H. Nguyen, R.D. Rauh, Electrodeposited iridium oxide for neural stimulation and recording electrodes, IEEE Trans. Neural Syst. Rehabil. Eng. 9 (2001) 2–11.

[27] G.T.A. Kovacs, C.W. Storment, J.M. Rosen, Regeneration microelectrode array for peripheral nerve recording and stimulation, IEEE Trans. Biomed. Eng. 39 (1992) 893–902.

Biographies

Damien C. Rodger received his BS degree in electrical engineering (magna cum laude with honors) from Cornell University in 2000. He is currently an MD/PhD candidate at the Keck School of Medicine of the University of Southern California and the California Institute of Technology conducting research in bioengineering on bioMEMS for ophthalmic and neural use. He held a Whitaker Foundation Graduate Fellowship from 2003 to 2006 and is a member of the IEEE EMBS and the Association for Research in Vision and Ophthalmology (ARVO).

Andy J. Fong received his MS degree in biomedical engineering at the University of California, Los Angeles in 2002. Currently he is pursuing his PhD in bioengineering at the California Institute of Technology. His dissertation research focuses on developing new technologies for treating spinal cord injury using a combination of robotically assisted physical rehabilitation, pharmacological treatments, and multi-locus electrical stimulation.

Wen Li received the BS degree in material science and engineering from Tsinghua University, Beijing, China, in 2001, the MS degree in microelectronics from Tsinghua University, Beijing, China, in 2003, and the MS degree in electrical engineering from California Institute of Technology in 2004. Currently, she is working toward a PhD in electrical engineering at the California Institute of Technology. Her research interests include flexible MEMS devices and systems for power and data transfer in retinal prostheses and other biomedical applications.

Hossein Ameri graduated from Tehran University of Medical Sciences in 1993. He received his Ophthalmology and Vitreoretinal Surgery training in Ireland and obtained his FRCSI from the Royal College of Surgeons in Ireland, and MRCOphth from the Royal College of Ophthalmologists in London in 2000. During his ophthalmology training at Cork University Hospital, he was also an official lecturer at University College Cork. He moved to the Doheny Eye Institute in Los Angeles in 2004 to pursue his research on retinal prostheses and retinal vascular disease. He is currently an assistant professor of ophthalmology at the University of Southern California.

Ashish K. Ahuja received his BS and MS degrees from Columbia University in applied physics and electrical engineering in 1999 and 2001, respectively. He worked in the Condensed Matter Physics Department at Bell Laboratories for 2 years. He then received his PhD in electrical engineering-electrophysics in 2007 from the University of Southern California. He is currently a Post-Doctoral Research Fellow at Second Sight Medical Products working towards the development of retinal prosthetic implants for the blind.

Christian Gutierrez received his BS degree in electrical engineering from the California Institute of Technology in 2005. He continued at Caltech and received his MS in electrical engineering in 2006. He is currently under fellowship pursuing a PhD in biomedical engineering at the University of Southern California. His research interest is in the development of novel MEMS devices with applications to medicine and he is currently involved in research for an intraocular retinal prosthesis.

Igor Lavrov received his MD in 1999 from Military Medical Academy and his PhD in 2002 from the Pavlov Institute of Physiology. In 2002 he joined the University of Louisville School of Medicine as a postdoctoral fellow, and in 2005 the laboratory of Dr. Edgerton at the University of California, Los Angeles. His research interests have been focused on understanding spinal cord functional organization and mechanisms of spinal cord reorganization after injury, artificial activation of spinal cord circuits responsible for locomotion, and developing rehabilitation strategies for spinal cord injury.

Hui Zhong received her MD in 1983 from Hebei Medical College. She has been at the University of California, Los Angeles since 1994. Currently, she is a project scientist in the Neuromuscular Plasticity Laboratory in the Brain Research Institute. Her research interest is neuromuscular plasticity after spinal cord injury.

Parvathy R. Menon is currently an undergraduate at the California Institute of Technology and will receive her BS in engineering and applied science in bioengineering in 2008. Prior to joining the Caltech Micromachining Group, she worked as an Axline Scholar in the Microdevices Lab of the NASA Jet Propulsion Laboratory. Additionally, she has worked in the Network Architecture Lab (NAL) of Intel Corporation and at the Oregon Graduate Institute (OGI). In the fall of 2009, she will be pursuing graduate studies in bioengineering or medicine.

Ellis Meng received her BS degree in engineering and applied science from the California Institute of Technology in 1997. She pursued her graduate studies in electrical engineering and received her MS in 1998 and PhD in 2003 at the same institution. She is now an assistant professor of biomedical engineering at the University of Southern California. In the National Science Foundation Biomimetic MicroElectronic Systems Engineering Research Center (BMES ERC) she is a Thrust Leader for Interface Technology and the Associate Director of Education and Student Diversity. She is a member of Tau Beta Pi, the American Society of Mechanical Engineers (ASME), the Society of Women Engineers (SWE), and the Association for Research in Vision and Ophthalmology (ARVO).

Joel W. Burdick received his BS in mechanical engineering from Duke University and MS and PhD degrees in mechanical engineering from Stanford University. He has been with the Department of Mechanical Engineering at the California Institute of Technology since May 1988. His current research interests include robotic locomotion, sensor based robot motion planning, multi-fingered robotic grasping, medical applications of robotics, applied nonlinear control theory, and neural prosthetics.

Roland R. Roy received the MSc and PhD degrees in exercise physiology from Michigan State University, East Lansing, in 1973 and 1976, respectively. He is currently a researcher in the Brain Research Institute, University of California, Los Angeles. His primary research interests concern the plasticity of the neuromuscular apparatus when subjected to a chronic increase (exercise, functional overload, hypergravity) or decrease (spinalization, immobilization, weightlessness, hind limb unloading, spinal cord isolation) in neuromuscular activity.

V. Reggie Edgerton received his PhD in exercise physiology from Michigan State University. He has been at the University of California, Los Angeles, since 1968 and is currently a professor in the Departments of Physiological Science and Neurobiology and a member of the Brain Research Institute. Dr. Edgerton's laboratory focuses on how, and to what extent, the nervous system controls protein expression in skeletal muscle fibers as well as how the neural networks in the lumbar spinal cord of mammals, including humans, control stepping and how this stepping pattern becomes modified by chronically imposing specific motor tasks on the limbs after complete spinal cord injury.

James D. Weiland received his BS from the University of Michigan in 1988. After 4 years in industry with Pratt & Whitney Aircraft Engines, he returned to Michigan for graduate school, earning degrees in biomedical engineering (MS 1993, PhD 1997) and electrical engineering (MS 1995). In 1999 he was appointed an assistant professor of ophthalmology at Johns Hopkins. Dr. Weiland is now the Director of the Intraocular Retinal Prosthesis Lab at the Doheny Retina Institute, and is an associate professor of ophthalmology and biomedical engineering at the University of Southern California. He is a member of the IEEE EMBS, the Biomedical Engineering Society, and the Association for Research in Vision and Ophthalmology.

Mark S. Humayun received his BS from Georgetown University in 1984, his MD from Duke University in 1989, and his PhD from the University of North Carolina, Chapel Hill in 1994. He finished his training by completing an Ophthalmology residency at Duke and a Fellowship in Vitreoretinal Diseases at Johns Hopkins Hospital. Currently, Dr. Humayun is a professor of ophthalmology, biomedical engineering, and cell and neurobiology at the University of Southern California. Dr. Humayun is the Director of the National Science Foundation Biomimetic MicroElectronic Systems Engineering Research Center (BMES ERC). He is also the Director for the Department of Energy Artificial

Retina Project that is a consortium of five Department of Energy labs and four universities, as well as industry.

Yu-Chong Tai received his BS degree from National Taiwan University, and the MS and PhD degrees in electrical engineering from the University of California at Berkeley. He is currently a professor of bioengineering and executive officer and professor of electrical engineering at the California Institute of Technology, and director of the Caltech Micromachining Laboratory. His current research interests include flexible MEMS, bioMEMS, MEMS for retinal and neural implants, parylene-based integrated microfluidics, neuroprobes/neurochips, and HPLC-based labs-on-a-chip.